Developmental hourglass: Confirmation by numerical evolution and elucidation by dynamical-systems theory

Takahiro Kohsokabe[1], Shigeru Kuratanai[1] and Kunihiko Kaneko[2]
1 Center for Biosystems Dynamics Research, RIKEN, Minatojima Minanimachi 2-2-3, Chuo Ward, Kobe, Hyogo, Japan
2 Niels Bohr Institute, University of Copenhagen, Blegdamsvej 17, 2100, København, Denmark

Abstract
Determining the general laws between evolution and development is a fundamental biological challenge. Developmental hourglasses have attracted increased attention as candidates for such laws, but the necessity of their emergence remains elusive. We conducted evolutionary simulations of developmental processes to confirm the emergence of the developmental hourglass and unveiled its establishment. We considered organisms consisting of cells containing identical gene networks that control morphogenesis and evolved them under selection pressure to induce more cell types. By computing the similarity between the spatial patterns of gene expression of two species that evolved from a common ancestor, a developmental hourglass was observed, that is, there was a correlation peak in the middle stage of development. The fraction of pleiotropic genes increased, whereas the variance in individuals decreased, consistent with previous experimental reports. Reduction of the unavoidable variance by initial or developmental noise, essential for survival, was achieved up to the hourglass bottleneck stage, followed by diversification in developmental processes, whose timing is controlled by the slow expression dynamics conserved among organisms sharing the hourglass. This study suggests why developmental hourglasses are observed within a certain phylogenetic range of species.

Introduction
Elucidating the possible relationships between evolution and developmental processes is a fundamentally unsolved issue in biology. Nothing to speak of those early works of 19th-century embryologists and evolutionists such as von Baer [1], Darwin [2], and Haeckel [3]; even today, the search for the general laws of the evolution of developmental processes remains one of the most important challenges in the field of evolutionary developmental biology. As a candidate for such a general law, the “developmental hourglass" model has gathered increased attention. According to the developmental hourglass model, multicellular species belonging to the same phylum have the highest embryonic similarity at a particular intermediate period of their development, when the morphological elements characterizing the phylum are formed.

The validity of the developmental hourglass model was first noted based on the coincidence between the phylotypic stage of vertebrates and the period of temporal and spatial progression of the hox genes [4,5,6] and has been quantitatively verified for various taxa by bioinformatics analyses over the past two decades (for chordates [7-12]; for echinoderms [13, 14, 15]; for arthropods [16, 17]; for nematodes [18, 19]; for mollusks [20] and also suggested beyond the animal kingdom, for flowering plants [21]; for fungus [22]). One may state that the observed data support a developmental hourglass, at least in some phyla.

Despite the growing evidence for the developmental hourglass model, whether it is just a contingency in the evolution of multicellular organisms or a necessity therein, is still in question. In other words, the possible mechanisms underlying the evolutionary acquisition of mid-embryonic conservation remain elusive. Recent experimental studies have concluded that the developmental hourglass is not sufficiently explained by fragility in the bottleneck stage [23, 24], but rather, developmental constraints or limitations on phenotypic variability are suggested to be the main driving force of the emergence of the

developmental hourglass [23,25]. The relevance of the self-organization processes to the formation of the hourglass was discussed (as well as the origin of the life cycle of multicellular organisms [26]), whereas there is no consensus on the mechanism for the developmental hourglass.

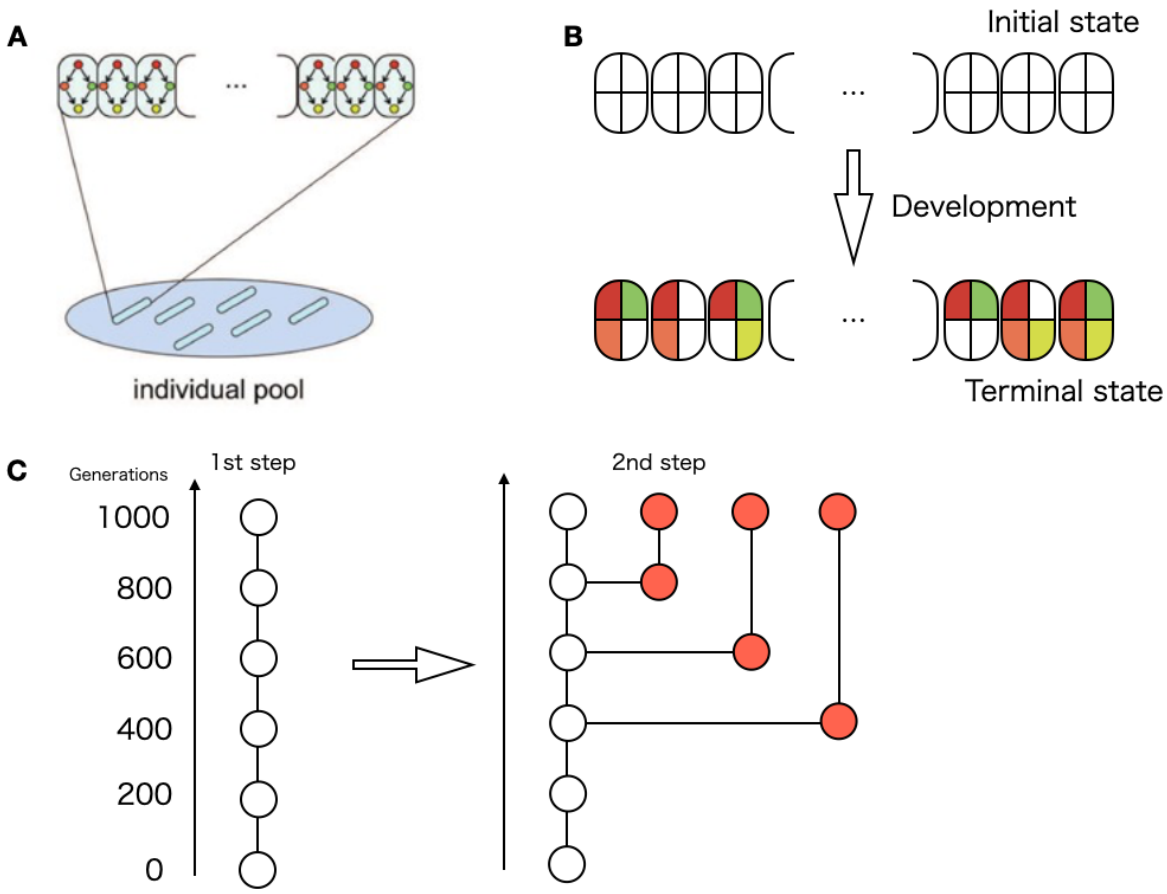

Figure 1. Schematic of the model used in this simulation

A: Each individual, which is a unit of selection, contains cells aligned in a one-dimensional space. These contained the same gene network. The state of each cell, given by the gene expression pattern, changes according to identical gene networks. There were 100 individuals in the evolving population in each generation.

B: Starting from the initial states, the gene expression patterns change according to the gene regulation network. After sufficient time, the expression of each cell reaches the terminal state, on or off.

Cell type was determined according to the on/off patterns of the target genes. For the four target genes, there were 2^4 possible states, as shown in the figure.

The fitness of an individual is determined by the number of different cell types in the terminal state. (In the figure, for instance, it is 6).

C: The selection procedure of species diverged from a common ancestor. The left chain represents the result of the first step of evolutionary simulation to select one species. Each circle represents the ancestor at each generation (although significantly abbreviated). As the second step, an ancestor at a certain generation was cloned and additional evolutionary simulations were carried from the ancestor up to the same generations of the original (1000).

Generally, it is challenging to solve such fundamental issue in the evolution of developmental processes by means of experimentally available data, and the search for mechanisms of the developmental hourglass is no exception. As another approach to this challenge, simulation studies on the evolution of developmental processes have been conducted over the past 20 years. In this case, one can repeat virtual evolution while retaining all the information, such as gene regulatory networks and developmental dynamics. Hypotheses about the possible relationships between development and evolution can then be tested. Theoretical hypotheses have been proposed using this approach regarding the structure of gene regulatory networks that induce segmentation [27, 28, 29], testing plausible evolutionary scenarios of segmentation mechanisms [30, 31], the relationship between developmental and mutational robustness [32], and congruence in the developmental and evolutionary processes in both RNA [33] and gene expression patterns [34].

In this study, we conducted an evolutionary simulation to investigate the mechanism behind the establishment of a developmental hourglass. For this purpose, we adopted a dynamical-system scheme to generate spatial patterns, which is commonly adopted in theoretical studies [27, 29, 30, 31, 34]. The model for the simulation can represent cellular states that are determined by gene expression patterns governed by gene regulatory networks and spatial cell-cell interactions, leading to the differentiation of cell types and pattern formation. Individuals must be selected according to a biologically relevant fitness function. We assumed that if there are more cell types within an individual, they attain more functions such that the fitness is higher. This fitness function reflects the idea that different cell types have different cellular functions, so that species with many cell types can deal with multiple tasks; hence, they are more adaptive than those with fewer cell types. Each cell type was defined according to the on or off state of the given output genes (see Fig. 1B for a schematic representation). In other words, our simulation mimics competition for survival, where individuals acquiring as many cell types as possible are the most adaptive and would leave more offspring.

To study the developmental hourglass, the developmental processes of extant species that diverged from a common ancestor must be compared. Thus, the model must represent not only a mother-to-daughter single-chain pedigree but also be able to examine a phylogenetic tree that contains multiple pedigrees as branches. To achieve this, a two-stage evolutionary simulation was performed. In the first stage, an evolutionary simulation of one lineage was performed to obtain one species by selection. In the second stage, evolutionary simulations were executed over the same number of generations, using an ancestor in the lineage of the first-step simulation. Using different random numbers for mutation, extant species branching from the common ancestor were obtained (see Fig. 1C for a schematic representation).

Using the above setup, we aimed to examine the correlation between gene expression patterns and the development of multiple species that diverged from a common ancestor. The results showed a developmental hourglass in the sense that the peak of such correlations lies in the middle of development. We also confirmed other reported characteristics, including accumulation of expressed pleiotropic genes and reduction of intra-species gene expression variance at the developmental bottleneck stage. The developmental period of the hourglass bottleneck obtained in the simulations was determined by the genes whose expression changed slowly during development, acting as genes to schedule development. The bottleneck serves as a developmental foundation that sufficiently attenuates the effects of the initial noise to prepare for subsequent developmental processes. Based on these results, the validity of the developmental hourglass and possible mechanisms for its emergence were discussed.

Results

Herein, we report the results of the simulation of a model based on the three policies described in the introduction. We assumed that the expression dynamics of each gene at each cell location are governed

by the gene regulation network (GRN), while some gene products diffuse through the space. The gene expression pattern in the model reached a fixed terminal state after sufficient 'developmental' time, where the expression of each gene reached an on or off state. Depending on the combination of on/off expression patterns of the given output genes, a cell type is determined (here we choose four output genes so that a maximum of 16 cell types could exist). Each cell type carries on some functions such that the fitness is given by the number of cell types that coexist over the space in the terminal state. GRNs with higher fitness than others will be selected with a higher probability, whereas slight random changes are introduced as "mutations" for replication to generate offspring. This simulation mimics evolutionary competition for survival, in which individuals that acquire as many cell types as possible are the most adaptive and leave more offspring. To represent multiple lineages that diverged from a common ancestor, additional evolutionary simulations of ancestral species were performed (see Methods for details).

Figure 2A shows specific examples of the developmental dynamics of two individuals acquired from evolutionary simulation after 1000 generations. The horizontal axis is the developmental time, and the vertical axis is the index indicating the cell location in a one-dimensional line. Different colours indicate different cellular states. The two individuals diverged from a common ancestral individual in the 800th generation. For precision, in this case, after selecting individual A1 in the primary simulation of 1000 generations, the ancestral individual of the 800th generation was chosen, and an additional simulation was performed over 200 generations (i.e., 1000 generations in total, equal to the generations in the primary simulation). Thus, owing to the secondary simulation, individual A2 was selected to represent different species that diverged from a common ancestor.

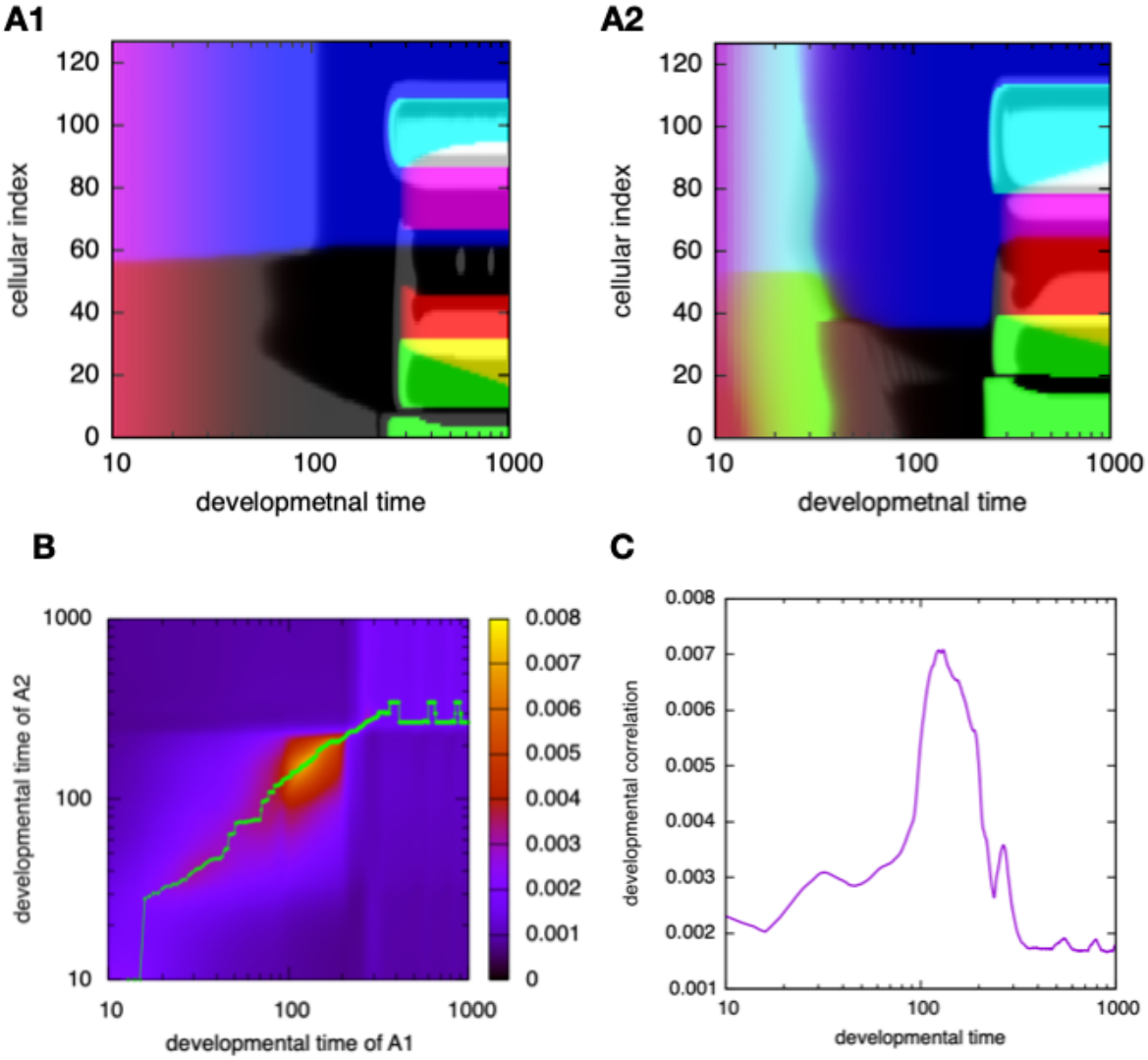

Figure 2. Examples of the evolutionary simulation that showed hourglass-like developmental correlation

A) Two examples of gene expression dynamics of evolved GRNs (A1, A2). The color represents the cellular state, i.e., the expression (On/Off) pattern of four output genes. The vertical axis is spatial index of cells and the horizontal axis is developmental time. Spatial pattern transitions were more frequent in the early developmental time, and a horizontal log plot was used to adequately depict them. This is consistent with experimental observations. Thereafter, the developmental time was plotted in logs. Following evolving 800 generations, the two GRNs evolved from a common ancestor of the 800th generation and then simulated further over 200 more generations, while suffering from different genetic changes, such that the two have diverged from the common ancestor.

B) The heat map of the similarity indicator, comparing the developmental dynamics of the two individuals given in A. The horizontal axis is the developmental time of A1, and the vertical axis is that of A2. Both axes are on a logarithmic scale. Each point indicates the similarity of gene expression states between the two examples at specific time points. (As the timescale of development can be different between the two in general, the comparison at different time points

is included. Note that the highest level of similarity appears in the middle stage. The green line indicates the locations where the similarity indicator takes maximum for each developmental time step of individual 1 (horizontal axis).

C) Projection of the similarity indicator on the green line in B against the developmental time of the first species (i.e., the horizontal axis in B).

By examining the development of spatial patterns with the differentiation of cell types, it was noted that there are some phases within which patterns change only slightly, and between them, drastic changes occur. Considering this case, there were three phases: early, middle, and late. By comparing the development of the two species, it may be difficult to judge at a glance in which phase the two are most similar to each other (Fig. 2A). Thus, we quantitatively compared the developmental processes of the two individuals to examine the similarity in patterns between them throughout the course of development. The differences in gene expression between the species were computed across each cell of the same spatial location, and the inverse of the sum of the differences was used as an indicator of the similarity in gene expression patterns between the two individuals. This indicator is similar to those used in experimental studies [9-15,18,19], in which the average expression over the whole cell is adopted by transcriptome analysis whereas it is superior in that it includes spatially local information. (Note, however, that the same result was obtained even if we adopted the spatially averaged indicator as adopted in the experiments (see supplementary figures SF1)
Fig. 2B displays the similarity between the gene expression states of individuals A1 and A2 at each developmental time. The indicator of similarity explained above was computed at each time point, as shown in the heat map. The horizontal axis represents the developmental time of individual A1, and the vertical axis represents that of individual A2. Fig. 2C displays the time course of similarity, which indicates that the peak of the similarity is in the middle of the developmental dynamics (see also Supplementary Figures SF2).

The similarity in gene expression patterns, as shown in Fig. 2B and 2C, can be calculated for any two species obtained in this simulation. Additional examples are shown in the supplementary figures SF2. As long as the compared species were phylogenetically close, we observed the peak of the similarity between two species that diverged from a common ancestor, always in the middle of developmental time, which is consistent with the developmental hourglass [9-15,18,19].

Next, we examined the phylogenetic range within which the above similarity peak was observed by comparing the two species that diverged from earlier common ancestors. Fig. 3 presents how the time course of the above similarity changes as the generations that the two species diverged earlier in the phylogenetic tree, where the similarity was computed between the original species and that departed at different branching points in the left phylogenetic tree (A, B, C). It was plotted against the developmental time of the original species, as shown in Fig. 2C.

The middle peak of developmental similarity was most prominent in comparison with the species departed at branch A (i.e. separated at the most recent 200th generation), and observed for B, albeit a bit weaker (separated at the 500 generations before), whereas in C, that is, the comparison between species separated much earlier in the tree (at the 800th generation), the middle peak disappears (see supplementary figure SF3, how the middle peak diminishes, as the point where the two species were increased per 100 generations). Hence, the similarity peak in the middle stage is preserved for comparison with the species that have diverged up to a certain depth range in the phylogenetic tree, but if they departed from a much farther ancestor, the peak disappeared.

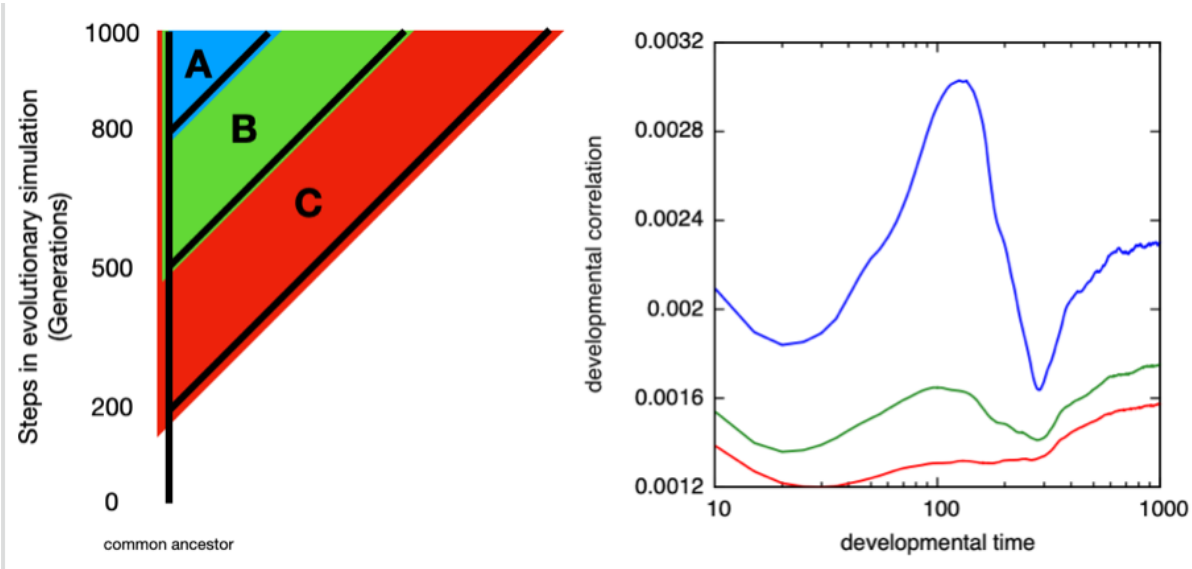

Figure 3. The similarity between two species that departed from a common ancestor at given earlier generations in the phylogenetic tree.

The similarity is computed as in Fig 1B and 1C, the average over pairs of individuals.

The horizontal axis represents the developmental time of the original species, and the vertical axis represents the similarity between the spatial patterns of gene expression. The line colour denotes how far the two species are, in comparison, branched in the left phylogenetic tree, diverged from the 800th generation A(blue), 500th generation B(green), and 200th generation C(red).

The horizontal axis was plotted on a logarithmic scale. At the middle developmental time, the similarity indicator takes a maximum when the pair branched at the later stage (In this case, for the pair branched at the recent 100–300 generations). Typically, the closer the phylogenetic pair of individuals, the more prominent the peak in the similarity indicator.

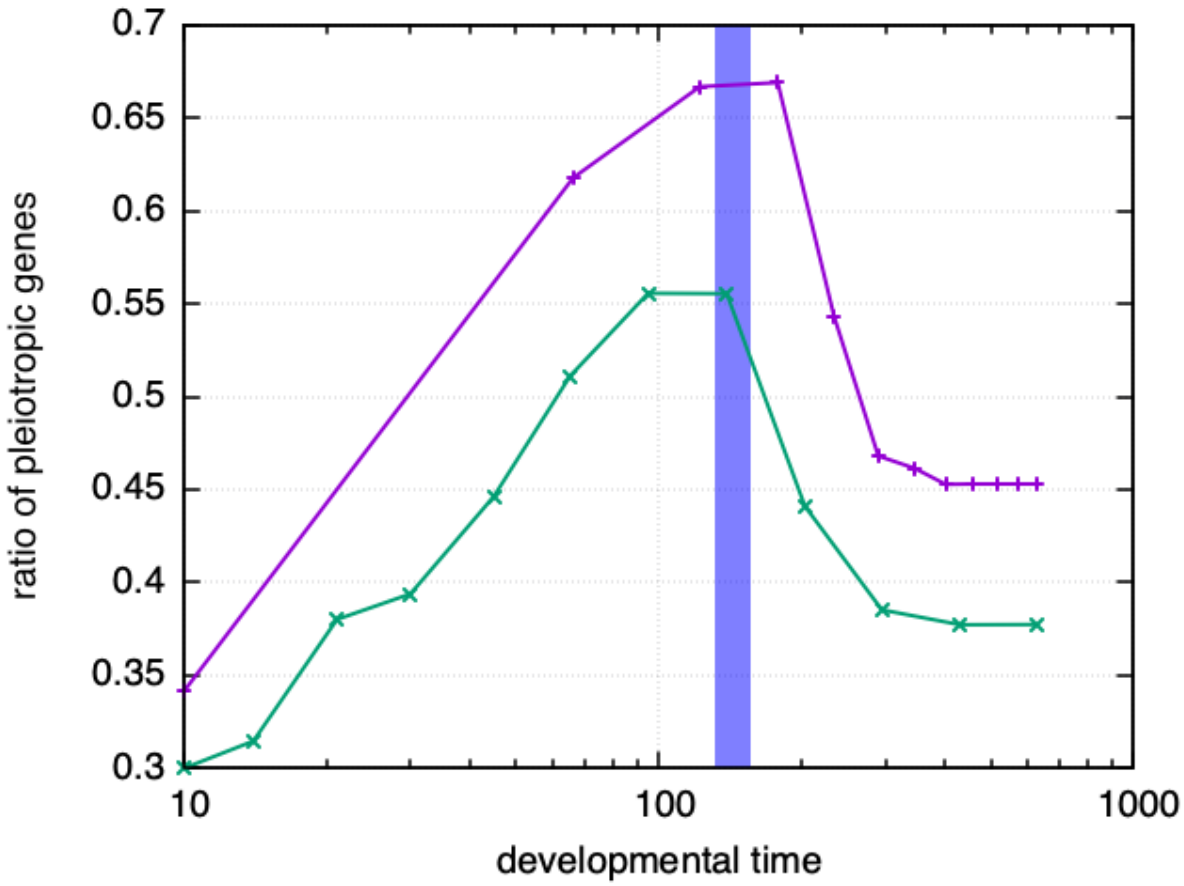

Figure 4. The time course of the fraction of the expressed pleiotropic genes. The pleiotropic genes are defined as those that are expressed for more than half of the developmental stages, whereas the stage was defined as splitting developmental time before reaching the stationary state into equal 12 spans, either by linear scale (the plot of purple (+) points) or by the logarithmic scale (the green(x) points). The fraction is obtained by averaging over 1000 individuals of different initial conditions, whereas the variance from the average was quite small. The area colored by blue indicates the typical range of developmental bottleneck (average ± standard deviation), which is given by comparison over other individuals diverted 200 generations earlier.

Next, we examined whether the present simulation results also contain other properties reported in the development of the hourglass-like conservation pattern.

In [35], it was observed that genes expressed in multiple stages during development (pleiotropic genes) were predominantly expressed at the bottleneck middle stage. Thus, we defined pleiotropic genes in our simulation and computed the ratio of the number of expressed pleiotropic genes to the total expressed genes. To compute it, we split developmental time into 12 stages and defined the "pleiotropic genes" as those that are expressed for more than half of the stages. Then the fraction of expressed pleiotropic genes at each stage was plotted over the developmental stages. As shown in Fig. 4, the fraction had a peak at the bottleneck time shown in the blue band. This increase of expressed pleiotropic genes is consistent with the

experimental data（even though one might see arbitrariness in the above criterion for pleiotropic genes, the maximal fraction of expressed pleiotropic genes at the bottleneck time is insensitive to the details of the criterion, such as the threshold to be judged as expressed, and the way of partition of developmental time to stages).

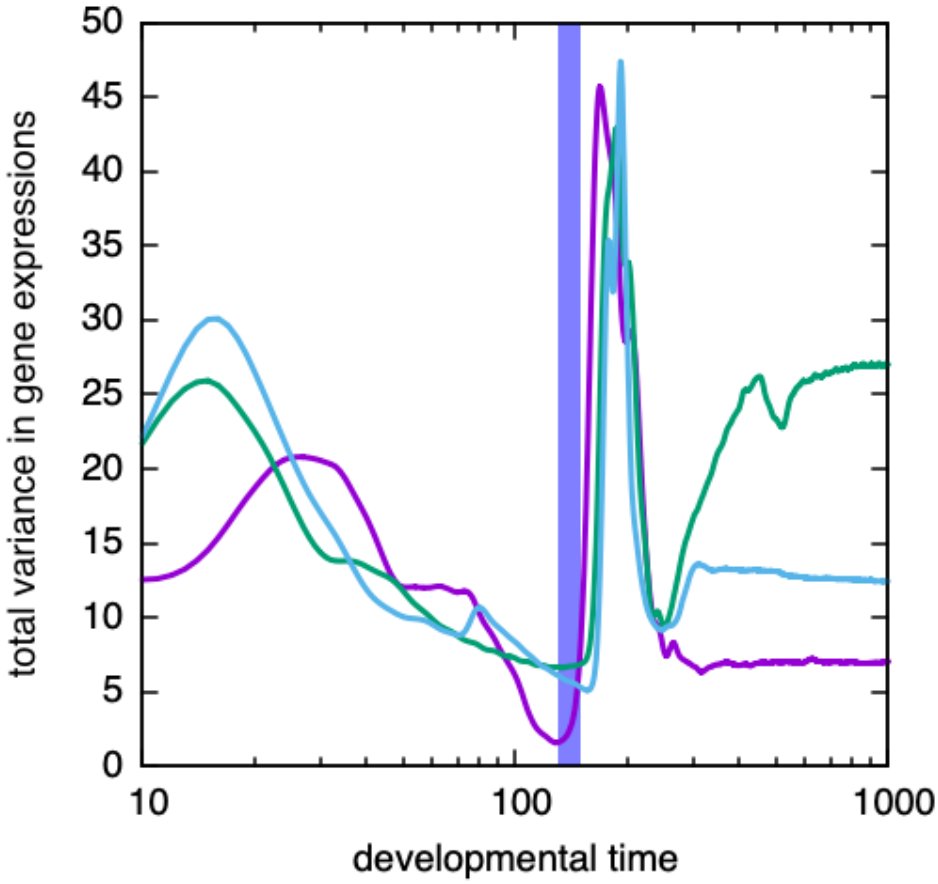

Figure 5. The variance of gene expression patterns over 1000 clones, i.e., those generated from the same genotype but with different initial conditions.
The horizontal axis represents developmental time, and the vertical axis represents the total variance of all genes in the cells. As specific examples, the data of three different individuals are indicated by different colours. The blue stripe indicates the typical range of observed developmental bottlenecks (average ± standard deviation), as obtained by comparing individuals belonging to blue triangle A in the phylogenetic tree in Fig. 3, which exhibits clear hourglass-like developmental correlations. Here, the initial conditions are chosen by adding Gaussian distribution noise with a variance $\sigma = 0.1$. (The details of the computation scheme are presented in the Methods section).

The recent experimental report shows that the difference in gene expression patterns between clones is minimal at the developmental hourglass's bottleneck [36,37]. We then tried to confirm if this characteristic is available from the simulation results and calculated the difference in the phenotypes (gene expression

patterns) of clones of the same species, due to variation in initial conditions. This phenotypic variation of clones (i.e., the averaged gene expression difference between individuals from the same species), was computed in our model by taking different initial conditions (see method) is shown in Fig. 4, against the developmental time in the logarithmic scale. The difference between individuals decreased up to a certain developmental time and then increased. The time that the variation took a minimum agrees with the time that the similarity in gene expression takes maximum, i.e., the bottleneck of the developmental hourglass (The drastic increase after the minimum is due to the difference in the timing when species-specific gene expression set in, as will be discussed later).

Note that the strength of the noise in the initial condition facilitates the emergence of a developmental hourglass. In this evolutionary simulation, the fitness is set up such that multiple cell types are generated in the final stage, under the variation in the initial state. The developmental process must reduce the initial variation to achieve robustness. Up to a certain developmental time, attenuation of the initial phenotypic variances by noise progresses. According to recent studies, this robustness to noise implies robustness to genetic changes [32]. Hence, during the developmental period, while the variance within the same species is reduced, the variation in expression among genetically different species is also reduced (as long as they are not too apart). This timing, in which the variance is minimized, agrees with the bottleneck in the hourglass (Fig. 4). Furthermore, if we evolve the system by reducing the variance of the initial conditions (or noise), then the developmental hourglass is no longer observed (see Supplementary Figure SF4).

In summary, our simulation reproduces the hourglass properties reported in real evolutionary developmental biology (evo-devo) data thus far, despite the simplification adopted in the model.

The developmental bottleneck and slow-gene control

Here, we note that the developmental similarity diagram (Fig. 2) drastically changes in the middle developmental period, where the pattern itself changes in a discrete manner, rather than continuously. Below, we explore how these drastic/discrete changes in development shape the developmental hourglasses.

Figure 6a illustrates examples of the changes in expression of each gene in one individual over the entire space. This figure also confirms the stepwise change. Furthermore, there is a stage in which the expression of many genes exhibits discrete changes (switches). This stage coincides with the bottleneck time of the hourglass. Before the bottleneck time, gene expression exhibited little spatial heterogeneity as shown in Fig. 6a. After the bottleneck, spatial subregions are generated in which specific genes are expressed and spatial heterogeneity is increased.

The time course of all gene expression levels for a given cell is shown in Fig.6b, which also demonstrates that the expression of various genes exhibits on/off switch changes around the bottleneck of the developmental hourglass stage. The expression levels of many initially expressed genes slowly decreased up to this bottleneck time, when fewer genes started to be expressed, depending on the space. (The timing of the expression of specific gene sets in varies by individual, which causes a drastic increase in phenotypic variance in Fig. 5).

The data also suggest the existence of a few genes whose expression levels change slower than those of the other genes. We computed the time scale of the expression changes of each gene (identical to the time for each gene that needs to change its expression from zero to fully expressed, or vice versa; see Methods for details) and plotted them in the order of their magnitude. As shown in Fig. 6c, there are a few (four in the figure) genes whose expression levels change much more slowly than others. In the present paper, they

are called ‘slow genes’. Such slow genes have also been observed in previous studies, which are key to relating the developmental timetable with evolutionary change, as they tend to control the expression of other genes whose expression levels change at a much faster time scale [34,38]. Furthermore, Fig. 6b suggests that the time scale of the slow genes is of the same order as the bottleneck time. This is reasonable because, with the time scale when expression levels of slow genes change, the expression of many other genes that are controlled by the slow ones are also switched between on and off.

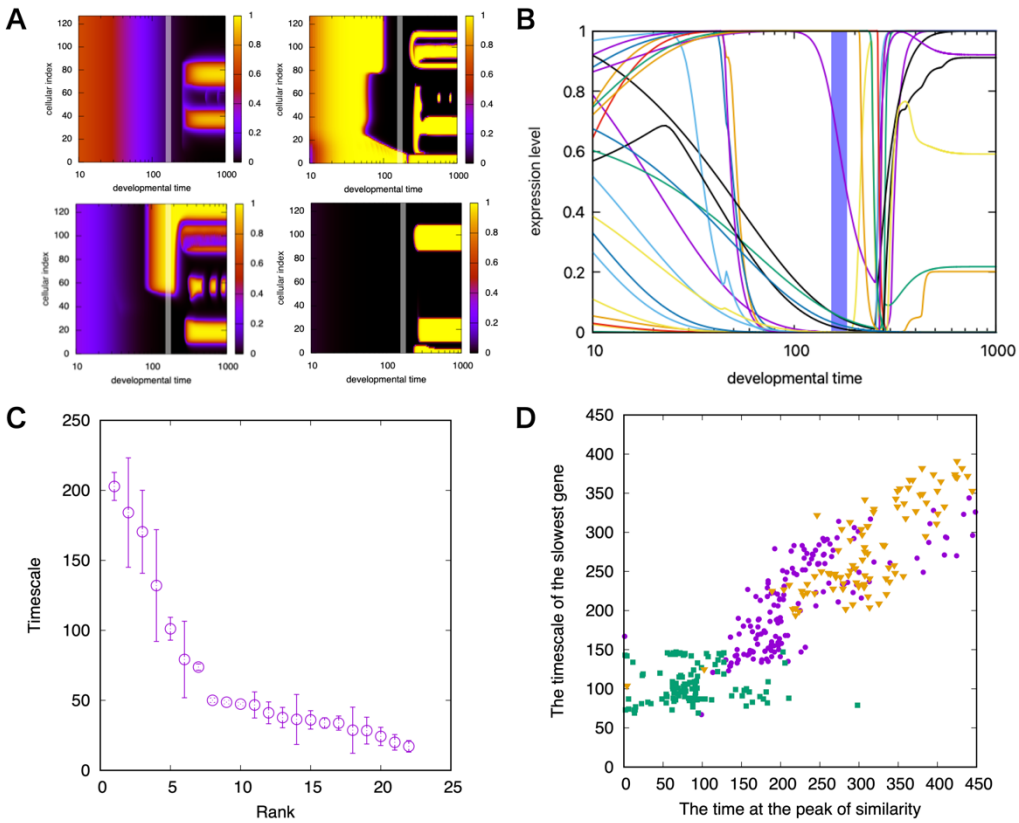

Figure 6. Control of the developmental schedule by slow genes

A: Examples of spatial gene expression dynamics. The gray vertical line in each figure is the timescale of the genes whose expression changes are slowest (see C and Methods). The left upper corner is the expression dynamics of the slowest gene.

B: Time series of expression levels of all genes at cell index 32 in A. Different colours correspond to the expression levels of different genes.

C: Time scale of expression changes of each gene, which is plotted in order as a function of its rank in magnitude. Error bars are the standard deviation of the timescale of genes. (For the computation of the timescale of genes, see Methods section).

D: Correlation between the timescale of the slowest gene and the timing of the bottleneck of the detected developmental hourglass. Blue circles represent data from the individuals acquired through evolutionary simulation, whereas green and light blue dots represent data obtained by adopting a parametric change to the slowest gene in the original (blue dots). Green squares represent the cases in which the timescale of the slowest genes was changed to five times faster, and the orange triangles represent those changed with ⅕ times slower (See also [38] and Supplementary figure SF5 for the heterochronic shift induced by manipulation of the slow gene).

In Fig. 6d, the correlation between the timescale of these slowly changing genes and the average bottleneck time of the developmental hourglass is plotted. These variables are linearly correlated. To confirm the linear relationship, we also created mutants in which the timescale of slow genes was altered and examined if the bottleneck time changed accordingly. A common linear relationship between the timescale of slow genes and the bottleneck time was confirmed (see Methods for the computation of the timescale of genes). Most individuals that shared a bottleneck in the developmental hourglass shared common slow genes. In contrast, the probability that two (distant) species that do not share the same hourglass of development have common slow genes is much lower, and at a chance level, that is, that for two randomly generated networks.

Discussion

In summary, our evolutionary simulation confirmed the developmental hourglass. When we compared species diversified from the common ancestor, we observed (i) amongst phylogenetically close species, the similarity in the gene expression patterns is maximal at the intermediate developmental period. Even though neither the initial population nor the fitness condition favors the developmental hourglass, it was spontaneously shaped through evolution. (ii) at this bottleneck period, the number of pleiotropic genes was at the maximum, and (iii) the individual variances in gene expression levels over clones were at the minimum. These three features agree quite well with those experimentally reported as the developmental hourglass. We then uncovered, at that stage, expressions of many genes are switched on or off, driven by a few genes whose expressions change slowly ("slow genes"). The timescale of the expression dynamics of these slow genes agrees with that of the bottleneck period.

To gain robustness in the developed pattern, the unavoidable variations that existed in the initial stage and throughout the development should be reduced. In our model, such reduction progresses up to the bottleneck stage, where the variation among individuals is minimized. This is consistent with the recent experimental report [36,37]. The developmental hourglass in our model is observed when the perturbations induced in the initial condition are sufficiently large.

In recent theoretical and experimental studies, the correlation between phenotypic variance by noise and that by genetic changes has been observed [32,39,40]. By extending the argument of such a correlation to the developmental time course, one may expect that the reduction of the initial variance by noise leads to a reduction in variance across genetically altered individuals. This explains the coincidence between the time of minimal variance over clones and the developmental bottleneck over genetically different species. Such a decreased variance at the bottleneck time was recently suggested [36,37].

At the bottleneck stage, the expression of slow genes sets in, and most genes change their expression levels. Following the expression of slow genes, the expression of other genes is diversified by species, leading to a developmental hourglass. The later developmental processes are contingent on the species. However, the mechanism driven by slow genes to absorb variations in the initial variation was preserved through evolution. Thus, the developmental hourglass is expected to be observed for species with the shared control mechanism mediated by slow genes.

In summary, the developmental hourglass obtained in our simulation results was caused by an attenuation of the variation in the initial state, accompanied by the expression of a few slow genes that control the developmental process. If these slow genes are conserved among species that diverged from the common ancestor, they share the common developmental bottleneck time determined by the slow genes.

If the two species diverted far earlier, the commonality of the slow genes would no longer be conserved.

Even though the attenuation of initial variation should be present, it would use different gene sets, the gene expression patterns of the two species would no longer be similar in the intermediate developmental stage, and the similarity indicator peak would no longer exist. Then, the similarity can be maximal either at the very beginning or the very last developmental time (Fig. 4). This result corresponds well with the cross-phylum comparison of gene expression patterns, as reported previously [41].

The slow genes regulate the expression of many other genes, as was shown previously [34]; thus, with this timescale of slow genes, many genes change their expression levels, including pleiotropic genes. This leads to an increase in the fraction of expressed pleiotropic genes in the developmental bottleneck period, which is consistent with the present simulation and experimental data [35]. The phylogenetically conserved time scheduling by slow genes can explain the range of species in which the hourglass was observed, which might correspond to the range within the same phylum. In the present simple model, morphogenesis is determined only by the expression of genes; thus, the control of development is regulated solely by gene expression, whereas development in real organisms includes other interactions due to cell motion, mechanical forces, among others. When such processes are included, the commonality of the slow control mechanisms explains the hourglass. In other words, species of the same phylum might be defined as those sharing a common slow control mechanism to reduce noise in the early developmental period. Exploration of common slow mechanisms across species sharing developmental bottlenecks would facilitate our understanding of hourglass phenomena.

The primary limitation of the study is that the model employed in this simulation is extremely simplified in terms of the number of genes and spatial degrees of freedom compared to real organisms. However, the synergy between gene expression dynamics and cell-to-cell diffusion is common in the development of real organisms [42]. In the present model, the collective movement of cells under mechanical forces was not considered. However, when represented mathematically, such mechanical processes can also be represented by a combination of gene expression dynamics and diffusive interactions among cells [43], and the basic results obtained in this study will be valid under the inclusion of such processes.

Methods

Model

The model in this study considered the evolution of a finite-sized population of 100 individuals. In each generation, individuals exhibit specific gene expression patterns according to gene expression dynamics with cell-cell interactions provided by their own gene regulation networks. According to the gene expression patterns of each individual, fitness is computed, and those with higher fitness will descend to the next generation. Those with higher fitness can produce multiple offspring, and those with lower fitness cannot, therefore 100 descendants are generated in total. Evolutionary simulations were conducted by iterating the scheme. This section provides a detailed description of our proposed model.

Gene regulation networks

In this study, the total number of genes in gene networks was fixed at N = 24, and gene regulation networks were described as an $N \times N$ matrix $J_{i,j}$, where the interaction between gene j and gene i is given by its (i, j) element. Interaction was represented as a discrete value of 1 (activation), -1 (inhibition), or 0 (no interaction between the two genes).

Gene expression dynamics

A cell's state is represented by the expression levels of N genes, that is, the number of expressed proteins. Here, let $x_i(r,t)$ be the protein expression level of the i-th gene in the r-th cell at time t. Cells are aligned in a 1-dimensional space. Proteins expressed from each gene either activate, inhibit, or do not influence

the expression of other genes or their own expression. We assumed that the change in the *i*-th protein expression level is given by the following reaction-diffusion equation:

$$\frac{\partial x_i(r,t)}{\partial t} = \gamma_i(F\big(i, \boldsymbol{x}(r,t) - x_i(r,t)\big) + D_i \frac{\partial^2 x_i(r,t)}{\partial r^2} \qquad (1)$$

$$F(i, \boldsymbol{x}(r,t)) = f(\textstyle\sum_j J_{i,j} x_j(r,t) - \theta_i) \qquad (2)$$

where $\boldsymbol{x}(r,t)$ is the vector which elements are $x_i(r,t)$. $x_i(r,t)$ in Eq.(1) represents the degradation of the *i*-th protein, with γi as its rate [27,44,45]. The expression level was scaled such that the maximum level was unity. The function $f(x)$ is similar to a step function, where the function approaches 1 as x is increased to the positive side, and approaches 0 as $x_i(l, t)$ decreases to the negative side; in other words, if the term $\sum_j J_{i,j} x_j\,(r,t)$ is sufficiently larger than the expression threshold θ_i, then $F\big(i, x(r,t)\big) \sim 1$, which indicates that the gene is going to be fully expressed; if it is smaller than θ_i, then $F\big(i, x(r,t)\big) < 1$, which indicates that the gene expression is suppressed. Here, we choose $f(x) = 1/(1 + e^{-\beta x})$ where β, which was set to 40, denotes the sensitivity of the expression at the threshold. In general, it is proportional to the Hill coefficient.

Generation and density of gene regulation networks

In this study, gene regulation networks were initiated using a semi-random generation process. For each element of the network matrix, interaction values of-1, 0, and 1 are assigned probabilities of 1/16, 7/8, and 1/16, respectively. The generated networks have network density, that is, the number of total connections divided by the total number of genes ~ 2, which is comparable to the real data [46-48].

Initial/boundary conditions

Morphogen gradients, which were introduced as the expression of genes #0 and #1, were supplied externally. Fixed linear morphogens were induced from both sides for cellular use, such that $x_0(r,t) = x_0(t) = (M - r)/M$ and $x_1(r,t) = r/M$. These gradients are not only present in the initial state but are invariant in time. We also evaluated a case involving a gradient with an exponential dependence in space, as $\propto exp(-l/\xi)$, but this condition did not alter the conclusions presented in this study.

For genes other than genes #0 and #1(i.e. genes #2, #3,...,#N), the expression levels of each gene were set to be spatially uniform and inherited from their ancestors. These values can be altered by mutations (as described later).

Discrete Neumann boundary conditions were adopted at both ends for this study, that is $x_i(1) = x_i(2)$ and $x_i(M-1) = x_i(M)$ for $i = 2,3,4,....N$.

Fitness function

We defined cell types according to the ON/OFF states of the designated four genes (genes #2 to #5 in the model). Specifically, if one gene's expression is over 0.99 (with the value range [0,1]), the gene is ON, whereas if it is less than 0.01, the gene is OFF. The number of existing cell types, N_t, was computed by sampling over cells. The fitness function is set to become higher as more cell types coexist.

The model can maximally generate $2^4 = 16$ cell types such that the fitness of individual i is defined as $f_i = N_t$. Hence, the fitness is maximal if 16 different cellular states exist in cells aligned in a one-dimensional space.

Selection

Whether an individual in a population is selected for the next generation is determined probabilistically.

The probability that one individual would be selected is given by its relative fitness to others, i.e., $e^{f_i}/\sum_j e^{f_j}$, for all *j*, where *i* and *j* are individual indexes.

Mutation

During the replication process, the gene network structure and parameters in the reaction-diffusion equation were slightly changed by the random mutation. Here is the list of evolvable parameters and their degrees of change during one replication.

Population cloning

Each evolutionary simulation was executed for up to 1000 generations, and we sampled cases in which the fitness of the fittest individual at the 1000th generation was above 15 (the maximum was 16). For these fitted individuals, we further cloned the ancestral populations. We selected ancestral populations from each 100th generation and evolved them up to 1000th generation. The parameters and mutational setups for the evolutionary simulations were identical to those of the original simulation.
Individuals obtained by these evolutionary simulations of the cloned population represent offspring that diverged from the same pedigree with different branching points.

Calculation of the similarity indicator of gene expression patterns

The similarity of gene expression patterns between two individuals was calculated using two indicators: Pearson's correlation coefficient and the inverse of the total gene expression difference. The definitions of the two indicators are as follows:

1) the inverse of the total gene expression difference

$$\Delta(t_1, t_2) = \frac{1}{\sum_i \sum_r |x_i^1(r, t_1) - x_i^2(r, t_2)|}$$

where $x_i^k(r, t)$ indicates gene i's expression level at location r, time t, of the individual k.

2) Pearson's correlation coefficient

For each developmental time t_1, t_2, the correlation coefficient $\rho(t_1, t_2)$ is given as

$$\rho(t_1, t_2) = \frac{cov(\boldsymbol{X}^1(t_1), \boldsymbol{X}^2(t_2))}{\sigma_{X^1(t_1)}\sigma_{\boldsymbol{X}^2(t_2)}}$$

where $\boldsymbol{X}^k(t)$ is the vector in which elements $X_i^k(t)$ are the summation of gene *i*'s expression over space in individual *k* at a given time *t*, that is, $X_i^k(t) = \sum_r x_i^k(r, t)$, is the standard deviation of X^k at time *t*, and *cov* denotes the covariance.

Calculation of variance in the pattern dynamics over clones

For a given individual, i.e., a set of GRN and parameters, *N* genetic clones are made while adding Gaussian noise to the original initial gene expression state of the development. The average and the standard deviation of the noise are 0 and 0.01, respectively. The developmental dynamics of those clones are calculated according to the same equation for gene expression dynamics. Then, the variance in the pattern dynamics over clones, which indicates how the initial difference propagates during development is calculated as

$$var(t) = \frac{1}{N}\sum_k \sum_r \sum_i (x_i^k(r, t) - \overline{x_i(r, t)})^2$$

Where *var(t)* indicates the developmental variance over clones at time *t*, $x_i^k(r,t)$ is the gene *i*'s expression in an individual *k*, at location *r* and time *t*. $\overline{x_i(r,t)}$ is the average of $x_i(r,t)$ over clones, i.e., $\overline{x_i(r,t)} = \frac{1}{N}\sum_j x_i^k(r,t)$

Calibration of the timescale of slow gene

To calibrate the timescale of genes, first, we defined the timestep. The timestep refers to an arbitral small interval of time. In this study, we adopted the timestep as the interval for the increment of time during the numerical simulation of gene expression dynamics. Similar calculations could be performed in actual experimental systems if the interval was chosen sufficiently small compared to the time needed for gene expression to saturate.

With the length of the timestep, we can estimate the partial derivative of gene expressions as $\left.\frac{\partial x_i(r,t)}{\partial t}\right|_{t=t_k} \sim \frac{x_i(r,t_k)-x_i(r,t_{k-1})}{\Delta t}$, where $x_i(r,t)$ is the gene expression level of gene *i* at location *r,* time *t.* Δt is the timestep and t_k indicates the time after the *k* timesteps, i.e., $t_k = k\Delta t$ (k = 1,2,...).

The timescale of genes can be calibrated by counting timesteps according to the following schema.

Count up *k* by 1 if the following two conditions are not violated.

1. The sign of the derivative at $t=t_k$ is the same as that of the time at t_{k-1}. i.e.,
$\frac{x_i(r,t_k)-x_i(r,t_{k-1})}{\Delta t}\frac{x_i(r,t_{k+1})-x_i(r,t_k)}{\Delta t} > 0$
2. The absolute value of the derivative at time t_k is bigger than a threshold, in this study we adopted the threshold as 0.001.
The condition 1 is for not counting oscillatory behavior and the condition 2 is for not counting time steps after saturation.

References

1 von Baer, K. E. U ̈ber entwickelungsgeschichte der thiere. Beobachtung und Reflexion, 1, (1828).

2 Darwin, C. On the Origin of Species by Means of Natural Selection, Or The Preservation of Favoured Races in the Struggle for Life. John Murray (1859).

3 Haeckel, E. Generelle morphologie der organismen. Allgemeine grundzu ̈ge der organischen formen-wissenschaft, mechanisch begru ̈ndet durch die von Charles Darwin reformirte descendenztheorie. G. Reimer (1866).

4 Slack, J., Holland, P. & Graham, C. The zootype and the phylotypic stage. Nature 361, 490–492 (1993).

5 Duboule, D. Temporal colinearity and the phylotypic progression: a basis for the stability of a vertebrate Bauplan and the evolution of morphologies through heterochrony. Development, 135-142 (1994).

6 Rudolf A. Raff. The Shape of Life: Genes. Development, and the Evolution of Animal Form. University of Chicago Press (1996).

7 Hazkani-Covo, E., Wool, D., & Graur, D. In search of the vertebrate phylotypic stage: a molecular examination of the developmental hourglass model and von Baer's third law. Journal of Experimental Zoology Part B: Molecular and Developmental Evolution, 304(2), 150-158 (2005).

8 Irie, N., & Sehara-Fujisawa, A. The vertebrate phylotypic stage and an early bilaterian-related stage in mouse embryogenesis defined by genomic information. BMC biology, 5(1), 1-8 (2007).

9 Irie, N., & Kuratani, S. Comparative transcriptome analysis reveals vertebrate phylotypic period during organogenesis. Nature communications, 2(1), 248 (2011).

10 Wang, Z., Pascual-Anaya, J., Zadissa, A. et al. The draft genomes of soft-shell turtle and green sea turtle yield insights into the development and evolution of the turtle-specific body plan. Nat Genet 45, 701–706 (2013).

11 Hu, H., Uesaka, M., Guo, S. et al. Constrained vertebrate evolution by pleiotropic genes. Nat Ecol Evol 1, 1722–1730 (2017).

12 Marlétaz, F., Firbas, P.N., Maeso, I. et al. Amphioxus functional genomics and the origins of vertebrate gene regulation. Nature 564, 64–70 (2018).

13 Malik, A., Gildor, T., Sher, N., Layous, M., & de-Leon, S. B. T. Parallel embryonic transcriptional programs evolve under distinct constraints and may enable morphological conservation amidst adaptation. Developmental biology, 430(1), 202-213 (2017).

14 Gildor, T., Cary, G.A., Lalzar, M. et al. Developmental transcriptomes of the sea star, Patiria miniata, illuminate how gene expression changes with evolutionary distance. Sci Rep 9, 16201 (2019).

15 Li, Y., Omori, A., Flores, R.L. et al. Genomic insights of body plan transitions from bilateral to pentameral symmetry in Echinoderms.Commun Biol 3, 371 (2020).

16 Domazet-Lošo, T., & Tautz, D. A phylogenetically based transcriptome age index mirrors ontogenetic divergence patterns. Nature, 468(7325), 815-818 (2010).

17 Kalinka, A. T., Varga, K. M., Gerrard, D. T., Preibisch, S., Corcoran, D. L., Jarrells, J., ... & Tomancak, P. Gene expression divergence recapitulates the developmental hourglass model. Nature, 468(7325), 811-814 (2010).

18 Levin, M., Hashimshony, T., Wagner, F., & Yanai, I. Developmental milestones punctuate gene expression in the Caenorhabditis embryo. Developmental cell, 22(5), 1101-1108 (2012).

19 Schiffer, P. H., Polsky, A. L., Cole, A. G., Camps, J. I., Kroiher, M., Silver, D. H., ... & Yanai, I. The gene regulatory program of Acrobeloides nanus reveals conservation of phylum-specific expression. Proceedings of the National Academy of Sciences, 115(17), 4459-4464 (2018).

20 Xu, F., Domazet-Lošo, T., Fan, D., Dunwell, T. L., Li, L., Fang, X., & Zhang, G. High expression of new genes in trochophore enlightening the ontogeny and evolution of trochozoans. Scientific Reports, 6(1), 1-10 (2016).

21 Quint, M., Drost, HG., Gabel, A. et al. A transcriptomic hourglass in plant embryogenesis. Nature 490, 98–101 (2012).

22 Cheng, X., Hui, J. H. L., Lee, Y. Y., Wan Law, P. T., & Kwan, H. S. A "developmental hourglass" in fungi. Molecular biology and evolution, 32(6), 1556-1566 (2015).

23 Zalts, H., & Yanai, I. Developmental constraints shape the evolution of the nematode mid-developmental transition. Nature Ecology & Evolution, 1(5), 0113 (2017).

24 Uchida, Y., Uesaka, M., Yamamoto, T., Takeda, H., & Irie, N. Embryonic lethality is not sufficient to explain hourglass-like conservation of vertebrate embryos. Evodevo, 9, 1-11 (2018).

25 Schmidt, K., & Starck, J. M. Testing evolutionary hypotheses about the phylotypic period of zebrafish. Journal of Experimental Zoology Part B: Molecular and Developmental Evolution, 316(5), 319-329 (2011).

26 Newman, S.A. Animal egg as evolutionary innovation: a solution to the "embryonic hourglass" puzzle. J. Exp. Zool., 316B: 467-483. (2011).

27 Salazar-Ciudad, I., Newman, S. A., & Solé, R. V. Phenotypic and dynamical transitions in model genetic networks I. Emergence of patterns and genotype-phenotype relationships. Evolution & development, 3(2), 84-94 (2001).

28 Salazar-Ciudad, I., Solé, R. V., & Newman, S. A. Phenotypic and dynamical transitions in model genetic networks II. Application to the evolution of segmentation mechanisms. Evolution & development, 3(2), 95-103 (2001).

29 François, P., Hakim, V., & Siggia, E. D. Deriving structure from evolution: metazoan segmentation. Molecular systems biology, 3(1), 154 (2007).

30 Fujimoto, K., Ishihara, S., & Kaneko, K. Network evolution of body plans. PloS one, 3(7), e2772 (2008).

31 Ten Tusscher, K. H., & Hogeweg, P. Evolution of networks for body plan patterning; interplay of modularity, robustness and evolvability. PLoS computational biology, 7(10), e1002208 (2011).

32 Kaneko, K. Evolution of robustness to noise and mutation in gene expression dynamics. PLoS one, 2(5), e434 (2007).

33 Ancel, L. W., & Fontana, W. Plasticity, evolvability, and modularity in RNA. Journal of Experimental Zoology, 288(3), 242-283 (2000).

34 Kohsokabe, T., & Kaneko, K. Evolution-development congruence in pattern formation dynamics: Bifurcations in gene expression and regulation of networks structures. Journal of Experimental Zoology Part B: Molecular and Developmental Evolution, 326(1), 61-84 (2016).

35 Hu, H., Uesaka, M., Guo, S., Shimai, K., Lu, T. M., Li, F., Fujimoto, S., Ishikawa, M., Liu, S., Sasagawa, Y., Zhang, G., Kuratani, S., Yu, J., Kusakabe, T. G., Khaitovich, P., & Irie, N. Constrained vertebrate evolution by pleiotropic genes. *Nature Ecology & Evolution*, *1*(11), 1722-1730 (2017).

36 Liu, J., Frochaux, M., Gardeux, V., Deplancke, B., & Robinson-Rechavi, M. Inter-embryo gene expression variability recapitulates the hourglass pattern of evo-devo. *BMC biology*, *18*(1), 1-12 (2020).

37 Uchida, Y., Shigenobu, S., Takeda, H., Furusawa, C., & Irie, N. Potential contribution of intrinsic developmental stability toward body plan conservation. BMC biology, 20(1), 82 (2022).

38 Kohsokabe, T., & Kaneko, K. Dynamical systems approach to evolution–development congruence: Revisiting Haeckel's recapitulation theory. Journal of Experimental Zoology Part B: Molecular and Developmental Evolution, 338(1-2), 62-75 (2022).

39 Landry, C. R., Lemos, B., Rifkin, S. A., Dickinson, W. J., & Hartl, D. L. Genetic properties influencing the evolvability of gene expression. Science, 317(5834), 118-121 (2007).

40 Tang, Q. Y., & Kaneko, K. Dynamics-evolution correspondence in protein structures. Physical Review Letters, 127(9), 098103 (2021).

41 Levin, M., Anavy, L., Cole, A. et al. The mid-developmental transition and the evolution of animal body plans. Nature 531, 637–641 (2016).

42 Green, J. B., & Sharpe, J. Positional information and reaction-diffusion: two big ideas in developmental biology combine. Development, 142(7), 1203-1211(2015).

43 Murray, J.D. Mathematical Biology. Springer (1989).

44 Glass, L., & Kauffman, S. A. The logical analysis of continuous, non-linear biochemical control networks. Journal of theoretical Biology, 39(1), 103-129 (1973).

45 Mjolsness, E., Sharp, D. H., & Reinitz, J. A connectionist model of development. Journal of theoretical Biology, 152(4), 429-453 (1991).

46 Serov VN, Spirov AV, Samsonova MG. Graphical interface to the genetic network database GeNet. Bioinformatics 14: 546-547 (1998).

47 Shen-Orr SS, Milo R, Mangan S, Alon U. Network motifs in the transcriptional regulation network of Escherichia coli. Nat Genet 31: 64-68 (2002)

48 Rosenfeld N, Alon U. Response delays and the structure of transcription networks. J Mol Biol 329: 645-654 (2003).

Supplemental Figures

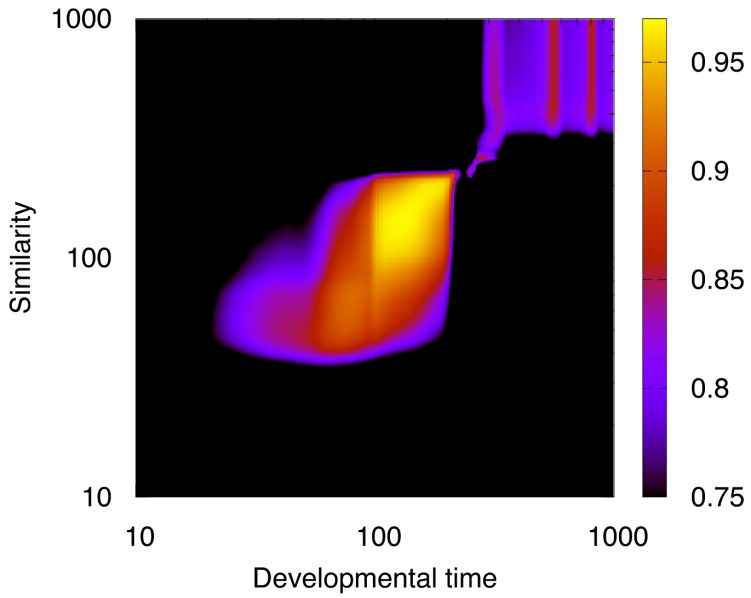

SF1 Developmental similarity of the examples in the main figure 1 measured by Pearson's coefficient
The similarity between the developmental dynamics of the two individuals shown in Fig.1A is represented as a heat map. The axes are the same as in Fig.1B and the similarity is measured by Pearson's coefficient.

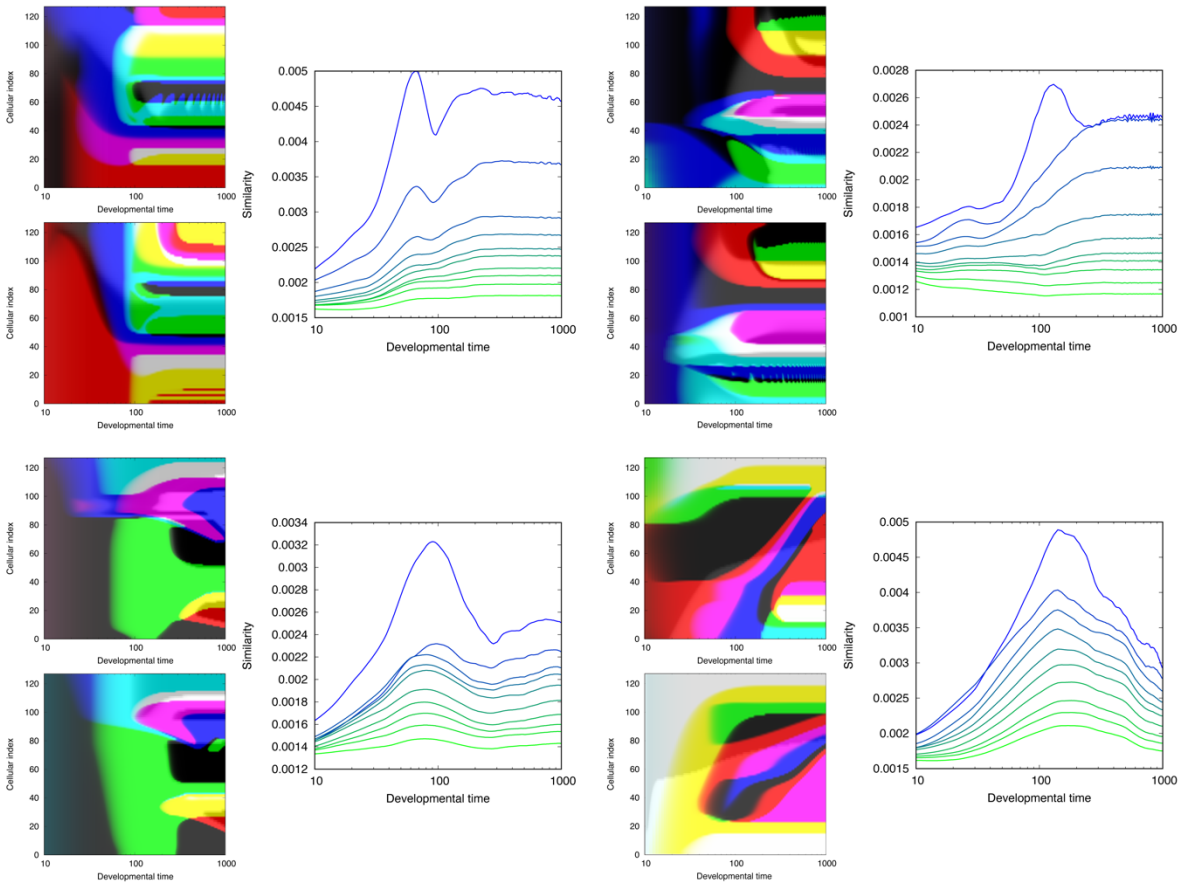

SF2 Additional examples that show developmental-hourglass-like similarity profile.
Four additional examples that show developmental hourglass are represented with developmental similarity. (Left) Two examples of gene expression pattern dynamics of evolved GRNs. The horizontal axis represents the developmental time, and the vertical axis represents the cellular index, i.e., space. (Right) The dependence of similarity is plotted against the developmental time, for species with different phylogenetic distance. The horizontal axis represents the developmental time, and the vertical axis represents the average of the similarity between the spatial patterns of gene expressions, in the same way as in Fig.2. The similarity is computed as in Fig.1C and averaged over pairs of individuals. The line colour denotes the phylogenetic distance of compared species departed from 900, 800,…, 100, 0 th generations. The similarity calculated among the species that diverged every 100 generations, from the 900th to the 0th generation is plotted.

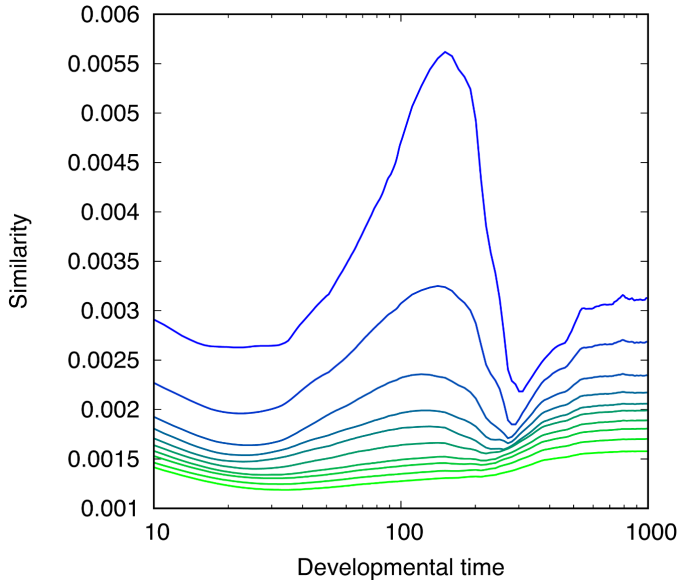

SF3 The time course of the similarity indicator and its dependence on the phylogenetic distance
Similarities among the species that diverged from a common ancestor are plotted, using the data from the same simulation run as in Fig.2, but plotted with phylogenic distance per 100 generations. Axes are the same as in Fig.2(left). Each curve represents the similarity among species that have different length of shared generations in the evolutionary path. The top blue curve represents the similarity of species that share 900 generations out of total 1000 generations, and with each 100 generations decrease of the length of shared generations, results are plotted as different colours, from blue to green (see also Fig.1 and Fig.2 for schematic representation).

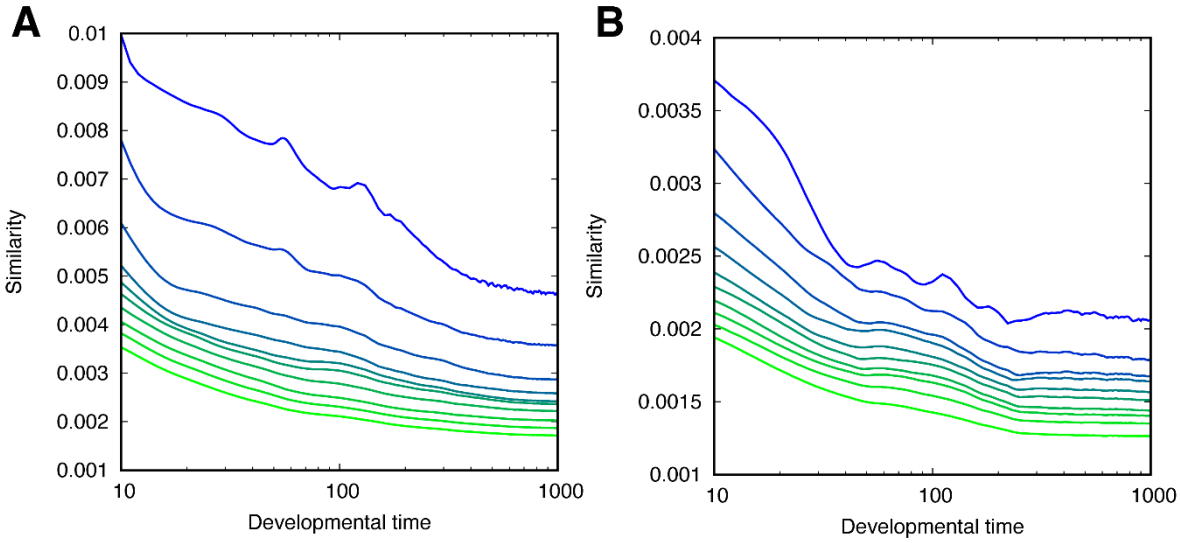

SF4 Examples of the similarity profiles with smaller noise levels for the initial condition
The relationship between phylogenetic distance and the value of the similarity indicator is represented as the same as Fig.2, SF2, and SF3 but with different noise levels on the initial condition. (A) An example of the case with the noise level on the initial condition $\sigma = 0.01$, which is 0.1 in the other figures. (B) An example of the case with the noise level on the initial condition $\sigma = 0.001$.

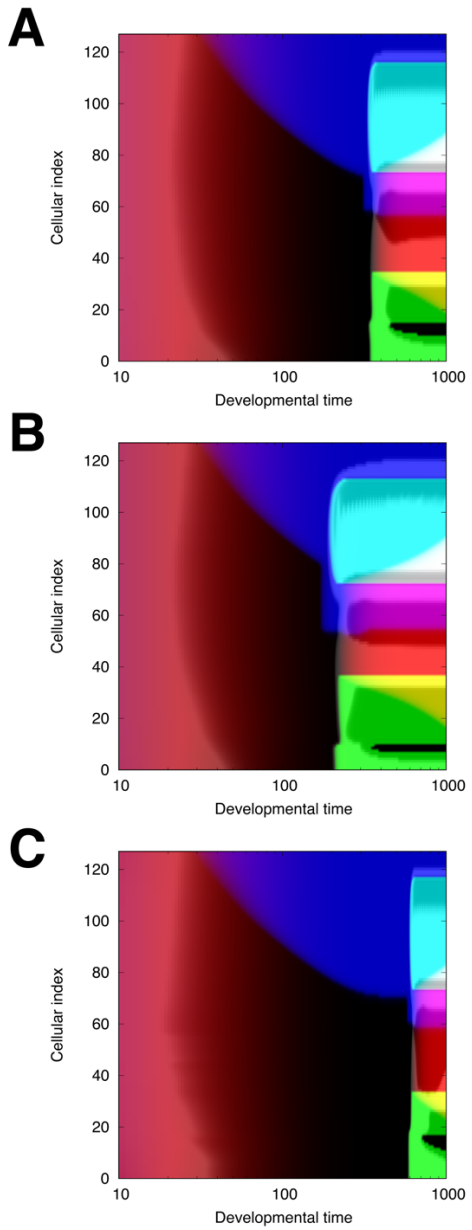

SF5 Slow gene control and heterochrony:
Subfigures A)–C) display pattern formation dynamics of the same gene network except for the change in the time-scale parameter of the slowest gene.
A: Pattern formation dynamics originally obtained from evolutionary simulation. The value of the timescale parameter of the slowest gene is 5.17×10^{-2}.
B: Pattern formation dynamics with a larger timescale of the slowest gene; 10.3×10^{-2}, 2 times larger than that of A.
C: Pattern formation dynamics with a smaller timescale of the slowest gene; 2.58×10^{-2}, 0.5 times smaller than that of A.